On Unsupervised Learning of Traversal Cost and Terrain Types Identification using Self-Organizing Maps*

Jan Faigl[0000−0002−6193−0792]* and Miloš Prágr[0000−0002−8213−893X]

Faculty of Electrical Engineering, Czech Technical University in Prague,
Technicka 2, 166 27, Prague, Czech Republic
{faiglj|pragrmi1}@fel.cvut.cz
https://comrob.fel.cvut.cz

Abstract. This paper reports on the deployment of self-organizing maps in unsupervised learning of the traversal cost for a hexapod walking robot. The problem is motivated by traversability assessment of terrains not yet visited by the robot, but for which shape and appearance features are available. The perception system of the robot is used to extract terrain features that are accompanied by traversal cost characterization captured from the real experience of the robot with the terrain, which is characterized by proprioceptive features. The learned model is employed to predict the traversal cost of new terrains based only on the shape and appearance features. Based on the experimental deployment of the robot in various terrains, a dataset of the traversal cost has been collected that is utilized in the presented evaluation of the traversal cost modeling using self-organizing map approach. In comparison with the Gaussian process, the self-organizing map provides competitive results and the found paths using the predicted traversal costs are close to the optimal path based on reference traversal cost of the particular terrain types. Besides, the self-organizing map can also be utilized for unsupervised identification of the terrain types, and it further supports incremental learning, which is more suitable for practical deployments of the robot in a priory unknown environments where reference traversal costs are not available.

1 Introduction

The work reported in this paper is motivated by a deployment of the multi-legged walking robot (depicted in Fig. 1) in an unknown environment, where the robot is requested to perform data collection missions or long-term environmental monitoring. In the motivational deployment, it is expected the robot continuously operates while it also improves its motion performance by avoiding hard to traverse areas. The robot can perceive its surrounding environment using

* This work was supported by the Czech Science Foundation under research project No.18-18858S. The authors acknowledge the support of the OP VVV MEYS funded project CZ.02.1.01/0.0/0.0/16_019/0000765 “Research Center for Informatics”.

its exteroceptive sensors such as RGB-D camera [18] while the proprioceptive signals (e.g., energy consumed, velocity, attitude stability) can be utilized to model the robot experience with the traversed terrain. A fundamental requirement to improve the robot motion performance is to avoid difficult terrains [2], and therefore, it is desirable to model the robot traversal cost and extrapolate the cost for seen but not yet visited areas to avoid costly terrains [11].

The herein reported empirical evaluation on unsupervised learning of the terrain traversability assessment is a part of our ongoing effort on terrain learning [10,12] for which we aim to develop computationally efficient unsupervised learning system to model and predict the robot traversal cost. Although models based on Gaussian Processes (GPs) [13] can be utilized for the traversal cost learning and prediction, e.g., modeling elevation maps [16], GP-based approach can be considered computationally demanding, and it does not scale with incremental deployment. In this paper, we focus on the evaluation of the Self-Organizing Map (SOM) [8] for unsupervised model learning and prediction of the traversal cost in a priory unknown environments, where the information about the ground truth traversal cost is not available. Based on our recent results on the evaluation of traversal cost learning reported in [4], we identified that combining data from similar terrain types might improve traversal cost estimates based on new exteroceptive measurements. Therefore, we employ SOM in traversal cost prediction, and we further investigate the clustering of the learned SOM [17] to identify prototypes corresponding to the similar terrain types. Moreover, the traversal cost defined as the attitude stability in [4] is extended by two additional cost indicators (the required power and achieved velocity) in the herein reported model learning, which supports the generalizability of the presented approach.

The remainder of the paper is organized as follows. A brief description of the addressed problem and utilized evaluation methodology is presented in the following section. The studied unsupervised terrain types identification is discussed in Section 3. The empirical results and description of the found evaluation insights are reported in Section 4. Concluding remarks are dedicated to Section 5.

2 Problem Specification

The addressed problem of traversal cost modeling follows our previous work reported in [4], and therefore, a brief problem specification is presented here to make the paper self-contained. The terrain characterization from exteroceptive measurements is described by the three shape features [9] and two appearance features of the ab channel means of the Lab color space. The exteroceptive feature descriptor $\boldsymbol{d}_{sa}$ is thus a vector $\boldsymbol{d}_{sa} = (s_1, s_2, s_3, a_1, a_2)$. In the learning phase, the descriptor is further accompanied by three traversal cost estimates c_1, c_2, and c_3, where c_1 is the mean value of the instantaneous power consumption, c_2 is the mean forward velocity, and c_3 characterizes the attitude stability determined as the variance of the robot roll; and all the cost indicators are computed from 10 s long period corresponding to the one motion gait cycle of

the multi-legged robot. The full descriptor $\boldsymbol{d}$ is thus eight dimensional vector $\boldsymbol{d} = (s_1, s_2, s_3, a_1, a_2, c_1, c_2, c_3)$.

The learning is performed for a sequence of descriptors called trail $\mathcal{T}$, e.g., $\mathcal{T} = (\boldsymbol{d}(1), \ldots, \boldsymbol{d}(n))$, to learn the traversal cost model $\mathcal{M}(\mathcal{T})$. The model is used to predict the traversal cost using a new exteroceptive feature $\boldsymbol{d}_{sa}$ that can be expressed as

$$(c_1, c_2, c_3) \leftarrow \text{predict}(\mathcal{M}, \boldsymbol{d}_{sa}). \tag{1}$$

For the traversability assessment of a new environment, the features correspond to a grid map of the environment. Hence, we consider the model evaluation for a set of m descriptors characterizing the new terrain $\mathcal{G} = \{\boldsymbol{d}_{sa}(1), \ldots, \boldsymbol{d}_{sa}(m)\}$.

Although a ground truth traversal cost is not available in the motivational deployment in a priory unknown environment, a reference value of the traversal cost can be considered for the evaluation of the selected unsupervised learning approaches. In the case labels of the particular terrain types in the trails used for the learning are available, e.g., provided by a human, the real measured traversal costs can be grouped for individual terrains, and "*ground-truth*" traversal costs can be estimated as the mean values of the traversal costs that can be further accompanied by the standard deviation. Thus, it is assumed the traversal costs are from normal distributions. However, such a reference value cannot be utilized for evaluation of the predicted traversal costs from explicitly unknown terrains, where the trails are not annotated, and thus the explicit terrain type labels are not available. In such a case, we can follow the approach based on the results reported in [4], and we can consider a GP-based model compound from the individual GPs for particular terrain types to model a probability distribution of the traversal costs per particular labeled terrain type. Since an individual GP is learned for each cost indicator and the terrain type trail, such a reference model is compounded from three times more GPs than the number of terrain types considered. Then, the compounded model can be utilized to provide a reference traversal cost for unlabeled data as the predicted traversal cost with the lowest variance of the predicted mean value.

The reference traversal cost model is denoted $\mathcal{M}_{\text{ref}}$ for the case of the mean and standard deviation values computed from the labeled trails, and $\mathcal{M}^{tt}_{\text{GP}}$ for the compounded GP-based model. The reference model $\mathcal{M}_{\text{ref}}$ can be used to estimate the traversal cost of the testing data $\mathcal{G}$, which consists of partially (human) labeled descriptors with the particular terrain types. For the unlabeled descriptors, the traversability cost is provided by the individual GP-based model with the lowest variance of the predicted mean value.

Even though we can utilize the root-mean-square error to evaluate the quality of the prediction, in a practical deployment, the traversal costs and also the exteroceptive descriptors are random variables. Therefore, we measure the performance of the model $\mathcal{M}$ by the ratio $R(\mathcal{M})$ defined as

$$R(\mathcal{M}) = \frac{|\{\boldsymbol{d}_{sa} | \boldsymbol{d}_{sa} \in \mathcal{G} \text{ and } |\,\text{predict}(\mathcal{M}, \boldsymbol{d}_{sa}) - \mu(\boldsymbol{d}_{sa})| \leq 2\sigma(\boldsymbol{d}_{sa})\}|}{|\mathcal{G}|} \cdot 100\%, \tag{2}$$

where $\mu(\boldsymbol{d}_{sa})$ and $\sigma(\boldsymbol{d}_{sa})$ correspond to the reference "*ground-truth*" if the terrain type for each $\boldsymbol{d}_{sa}$ is known, or they are provided by the compounded GP-based model $\mathcal{M}^{tt}_{\mathrm{GP}}$. The ratio R is motivated to measure "correctness" of the predicted values according to the reference model, where the prediction is considered correct if it fits about 95% values of the reference GP-based model prediction, and thus the ratio (2) is called the *correctness ratio*.

3 Unsupervised Terrain Types Identification

Even though we can imagine explicit terrain labels, e.g., flat ground and grass, the robot does not have such explicit terrain types when it is deployed in an unknown environment where it can only see its surroundings and perceive the terrain by the proprioceptive measurements. Therefore, we can imagine that similar terrain features can belong to the same "terrain type", and thus we can perform unsupervised clustering of the data to identify similarities.

For the SOM, we can consider a visualization of the learned lattices, e.g., using U-matrix [15]. Besides, we can also cluster the learned prototypes according to the smallest cluster separation measure [3] as suggested in [17]. In particular, we consider 2–30 clusters determined by 100 iterations of [7] initialized by [1]. The number of determined clusters can be considered as the number of terrain types in the dataset used for the learning. We propose the following procedure to evaluate the unsupervised identification of the terrain types.

First, we consider the dataset trail $\mathcal{T}$ is annotated by a human operator who provides explicit terrain type labels. The clusters of SOM prototypes are then examined for the terrain labels using the annotated descriptors of the trail $\mathcal{T}$. The learned prototypes do not precisely match the descriptors of $\mathcal{T}$ because of learning error, and therefore, we propose to annotate each prototype according to the label of the closest $d \in \mathcal{T}$. Thus, for each cluster, we compute a histogram of the specific terrain types of the given labels, and the cluster can be labeled according to the terrain type with the largest histogram bin. However, the robot experience with the terrain captured by the descriptors in $\mathcal{T}$ can be different from the human labels, and we can also expect a different number of clusters than the number of labels provided by the human. Therefore, we evaluate the identified terrain types as the percentage ratio of each terrain type label within each particular cluster and the total number of the clustered prototypes.

Let the total number of prototypes be M, the number of clusters be N, and the number of prototypes within the i-th cluster be m_i; then, the percentage ratio $T_{i,l}$ of the terrain type label l in the cluster i is computed as

$$T_{i,l} = \frac{|\{\boldsymbol{w} | \boldsymbol{w} \in \mathcal{N}_i, \text{ such that } \mathit{label}(\mathrm{argmin}_{\boldsymbol{d}\in\mathcal{T}}(\|(\boldsymbol{w}, \boldsymbol{d})\|)) \text{ is } l\}|}{M} \cdot 100\%, \quad (3)$$

where $\mathcal{N}_i$ is the i-th cluster of all prototypes in the SOM lattice $\mathcal{N}$, i.e., $\mathcal{N}_i \subseteq \mathcal{N}$, and $\mathit{label}(\cdot)$ is the label of the corresponding descriptor $\boldsymbol{d}$ of the trail $\mathcal{T}$. Since the sum of all $T_{i,l}$ gives one hundred percentage points, the ratios $T_{i,l}$ describe

a distribution of the human labels across the terrain types identified by the unsupervised procedure.

A similar evaluation can be directly performed on the trail descriptors using the same hierarchical clustering as for the SOM prototypes. Notice that the number of prototypes of the learned SOM is considerably smaller than the size of the input dataset, and thus continuous clustering of the trail descriptors can be demanding for a practical deployment with online learning. The evaluation results on the collected dataset with the real hexapod walking robot are reported in the following section.

4 Results

Individual trails for seven particular terrain types have been collected with the real hexapod walking robot. These trails are combinations of flat terrain and wooden blocks that are further covered by artificial turf and black fabric, which change the visual appearance of the terrain and impact the traversal costs, see Fig. 1. In addition, the seventh terrain is a wooden sloped surface with a visual appearance similar to wooden blocks.

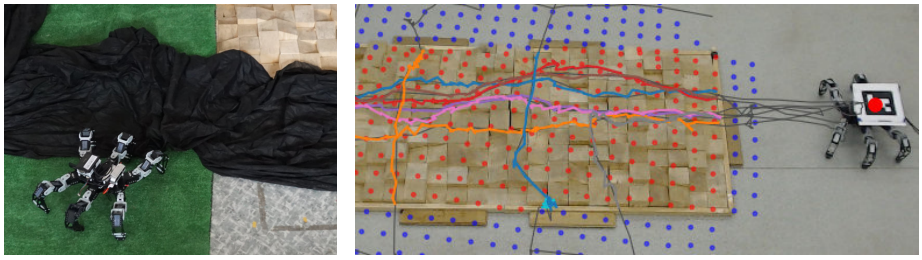

Fig. 1. Utilized hexapod walking robot and terrains types – flat floor and wooden blocks considered uncovered but also covered by artificial turf and black fabric. The terrain types are further accompanied by a single wooden sloped surface (not shown in the photo). The parts of the labeled trail on wooden blocks are visualized as color curves. The unlabeled descriptors are small blue disks.

Since an explicit human label of the terrain types is available, we can compute the "*ground-truth*" reference traversal costs as mean values accompanied by the standard deviations from all measured traversal costs indicators per individual terrain types. The particular reference costs are depicted in Table 1 where the forward velocity c_2 and attitude stability c_3 costs are multiplied by 100 to scale them to a competitive value to the power cost c_1 because their absolute measured values are relatively small. From the listed values, we can notice that some of the terrains are equal regarding the required energy cost c_1, such as wooden blocks covered by artificial turf and flat floor, which is because of the employed adaptive locomotion control [5], but the stability of the motion (captured by the cost c_2) differs. On the other hand, the most energy demanding terrains are flat floor covered by black fabric, which causes slippage

Table 1. Reference Traversal Costs – Average measured traversal cost values

Terrain	$\mathbf{costs}_{average}$			$\mathbf{costs}_{std.dev.}$		
	$\overline{c_1}$	$\overline{c_2}'$	$\overline{c_3}'$	σ_{c_1}	σ'_{c_2}	σ'_{c_3}
flat floor covered by black fabric	13.2	1.6	2.2	0.75	0.57	0.99
wooden blocks covered by black fabric	11.0	1.5	2.2	0.68	0.62	0.74
wooden blocks	11.1	1.7	2.2	0.64	0.68	0.76
wooden blocks covered by artificial turf	10.7	1.6	1.9	0.54	0.47	0.68
flat floor	10.6	2.3	0.9	0.85	0.53	0.22
wooden sloped surface	13.3	1.9	2.4	0.77	0.92	1.12
flat floor covered by artificial turf	10.6	1.8	1.0	0.37	0.65	0.23

Presented values for c_2 and c_3 are multiplied by 100 because absolute measured values are relatively small.

of the foot end-points, and wooden sloped surface. The increased slippage of these terrains corresponds to the relatively small velocity c_2 and high instability of the motion c_3. Regarding the navigation and avoiding difficult terrains, the most distinguishable real measured values are for the energy consumption c_1, which is thus suitable for weighting the traversed distance in the path planning. However, the weights of individual traversal costs can be further tuned according to a particular deployment scenario.

In addition to the direct computation of the reference model $\mathcal{M}_{\text{ref}}$, the compound GP-based reference model $\mathcal{M}_{\text{GP}}^{tt}$ is learned from the labeled trails, but all these trails are concatenated into a single trail $\mathcal{T}_{all}$ with 2177 feature descriptors for the evaluation of the learned GP and SOM from the unlabeled data. The evaluation is performed for the testing set $\mathcal{G}$ with 4355 descriptors from which only 1153 are labeled by the terrain type. The correctness ratio (2) computed only from the labeled test descriptors is thus denoted $\mathcal{R}$, and the ratio computed from all descriptors is denoted $\mathcal{R}_{all}$.

The standard SOM [8] with the three sizes of the squared lattice (10×10, 20×20, and 30×30) is utilized with the initial learning gain $g_0 = 10$ and the fixed learning rate $\mu = 0.99$. The gain is decreased $g \leftarrow (1 - \alpha)g$ after each learning epoch according to the gain decreasing rate $\alpha = 0.05$. A single learning epoch is considered as the adaptation of SOM to all input terrain descriptors (in random order), and the total number of learning epochs is limited to 300. The descriptors are used as they have been computed from the measured signals without any normalization.

The SOM learning procedure has been implemented in C++ and learning the complete model for $\mathcal{T}_{all}$ takes about 1.1 s, 3.9 s, and 8.6 s depending on the lattice size using the Intel i7-8550U CPU. GP-based learning utilizes GPy [6] and it takes about 113.9 s to learn $\mathcal{T}_{all}$ within the same computational environment. The prediction of the cost for a single feature using SOM is negligible as it takes about 0.5 μs, 2.0 μs, and 4.5 μs depending of the lattice size, while a single cost prediction using GP-based model takes about 8.7 ms.

First, the prediction of the learned SOM has been compared with the GP-based models using the correctness ratio (2) and the reference models $\mathcal{M}_{\text{ref}}$

Table 2. Correctness ratios R for labeled data of $\mathcal{T}_{all}$

Ratio	Cost	Model learned from $\mathcal{T}_{all}$							
		$\mathcal{M}_{\mathrm{GP}}^{tt}$	$\mathcal{M}_{\mathrm{GP}}$	$\mathcal{M}_{\mathrm{SOM}}^{10\times10}$	$\mathcal{M}_{\mathrm{SOM}}^{20\times20}$	$\mathcal{M}_{\mathrm{SOM}}^{30\times20}$	$\mathcal{M}_{\mathrm{SOM}_3}^{10\times10}$	$\mathcal{M}_{\mathrm{SOM}_3}^{20\times20}$	$\mathcal{M}_{\mathrm{SOM}_3}^{30\times30}$
R - $\mathcal{M}_{\mathrm{ref}}$	c_1	80.1	56.3	78.2	75.3	77.3	87.5	83.9	73.4
	c_2	78.6	78.0	89.0	85.0	85.0	85.3	85.9	73.5
	c_3	91.6	89.8	73.0	72.5	72.5	73.4	86.4	73.5
R - $\mathcal{M}_{\mathrm{GP}}^{tt}$	c_1	-	42.6	48.1	45.5	45.8	59.8	61.5	59.7
	c_2	-	69.7	77.3	75.7	74.5	79.2	81.7	80.4
	c_3	-	46.7	61.3	57.6	50.6	69.4	66.1	64.5

and $\mathcal{M}_{\mathrm{GP}}^{tt}$. Two types of prediction using the learned SOM are considered. The prediction using the closest prototype is denoted $\mathcal{M}_{\mathrm{SOM}}$. Besides, we consider prediction using the weighted average from k closest prototypes. Based on the empirical evaluation, we found that the best performance is for computing the average from three closest prototypes, and therefore, we report only results for $k = 3$ that are denoted $\mathcal{M}_{\mathrm{SOM}_3}$. Since SOM is randomized, the correctness ratios are computed from 20 trials, and the average values for the labeled data are reported in Table 2 and for the unlabeled data in Table 3, where the lattice size is encoded in the superscript. The standard deviations are in units of percentage points of the average values, and thus they are omitted for clarity.

Table 3. Correctness ratios R_{all} for unlabeled data using the reference $\mathcal{M}_{\mathrm{GP}}^{tt}$

Ratio	Cost	Model learned from $\mathcal{T}_{all}$						
		$\mathcal{M}_{\mathrm{GP}}$	$\mathcal{M}_{\mathrm{SOM}}^{10\times10}$	$\mathcal{M}_{\mathrm{SOM}}^{20\times20}$	$\mathcal{M}_{\mathrm{SOM}}^{30\times20}$	$\mathcal{M}_{\mathrm{SOM}_3}^{10\times10}$	$\mathcal{M}_{\mathrm{SOM}_3}^{20\times20}$	$\mathcal{M}_{\mathrm{SOM}_3}^{30\times30}$
R_{all}	c_1	46.7	51.5	50.8	51.3	56.0	56.8	56.6
	c_2	76.4	82.3	79.7	78.9	83.1	83.8	83.1
	c_3	55.5	56.4	55.2	49.1	60.7	59.9	58.4

The achieved correctness ratios reported in Table 2 and Table 3 indicate that all predictors provide competitive performance. Although a better performance is indicated for the reference "*ground-truth*" model $\mathcal{M}_{\mathrm{ref}}$ than for the compounded GP-based model $\mathcal{M}_{\mathrm{GP}}^{tt}$, explicit terrain types might not be available for deployment scenarios in a priory unknown environments. Therefore the compounded model is suitable for the evaluation of learned models without labeled trails shown in Table 3, because it provides the best performance for the labeled trails, see Table 2. The weighted average from three closest prototypes $\mathcal{M}_{\mathrm{SOM}_3}$ provides noticeably better prediction than $\mathcal{M}_{\mathrm{SOM}}$. On the other hand, increasing the size of the lattice does not improve the prediction correctness, and thus small and less computationally demanding 10×10 large SOM is sufficient.

The prediction correctness ratios vary for the individual traversal costs c_1, c_2, and c_3, and there is not a single best performing model among the performed trials of the SOM. Therefore, we select the particular learned model $\mathcal{M}_{\mathrm{SOM}_3}^{10\times10}$ with $R(c_1) = 64.7\%$, $R(c_2) = 79.3\%$, and $R(c_3) = 71.0\%$ for further investigation of the unsupervised terrain types identification using SOM. Similarly, we

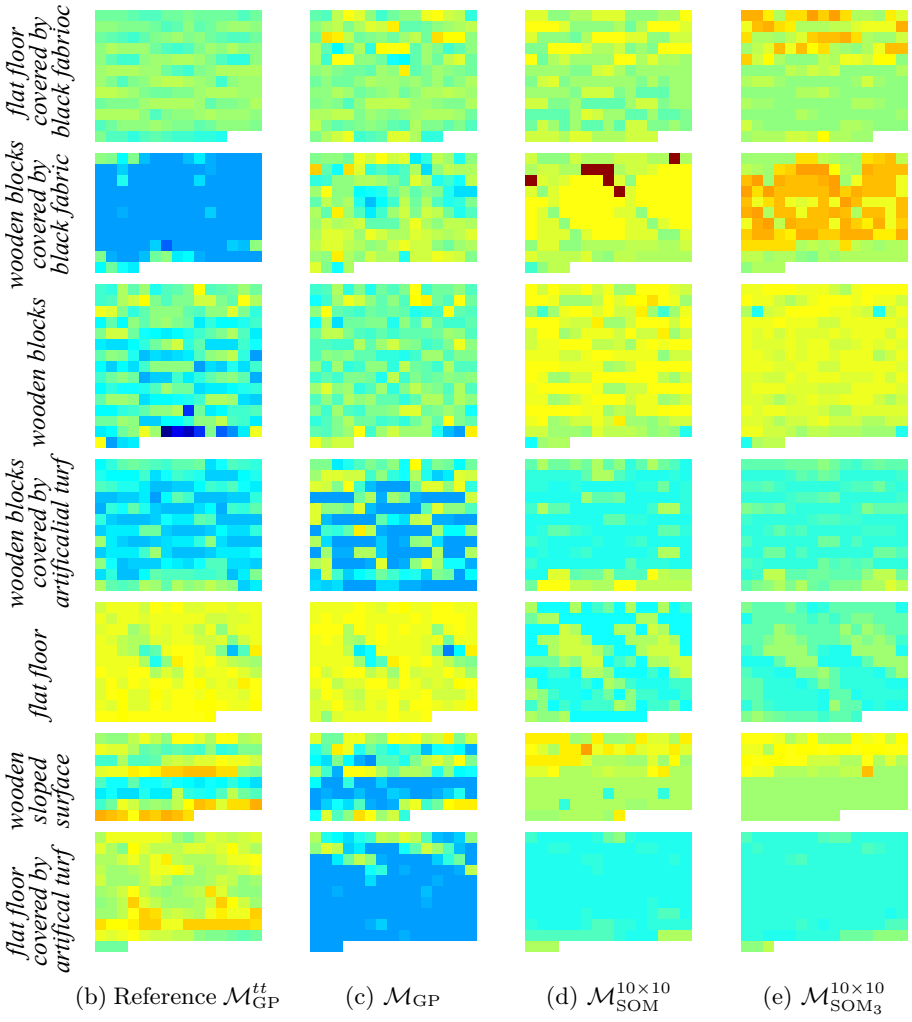

Fig. 2. Predicted values of the velocity cost c_2 for the labeled part of the testing data $\mathcal{G}$ that are organized into separate (possibly) equally large grids according to the particular terrain types from top to down as *flat floor covered by black fabric*, *wooden blocks covered by black fabric*, *wooden blocks*, *wooden blocks covered by artificial turf*, *flat floor*, *wooden sloped surface*, and *flat floor covered by artificial turf*. The absolute values of the prediction c_2 are colorized using the jet color palette (low values are in the blue and high values are in the red).

select $\mathcal{M}_{\mathrm{SOM}}^{10\times10}$ with $R(c_1) = 47.5\%$, $R(c_2) = 75.4\%$, and $R(c_3) = 63.2\%$ that is used for detail examination of the predicted values, which is shown in Fig. 2 for the expected velocity cost c_2 on the testing grid $\mathcal{G}$. Notice, that even though the prediction is not perfect regardless of the GP or SOM method, for the motivational deployment in path planning to avoid hard to traverse regions, the main

important property of the traversal cost prediction is distinguishability of the hard to traverse areas, which seems satisfiable for all the predictions and it is further detailed in the following section.

4.1 Predicted Traversal Cost in Path Planning Scenario

The possible impact of the traversal cost prediction to navigation of the robot in the environment is related to the ability to avoid hard to traverse areas, which is also related to the absolute values of the traversal cost and the computed distance cost in the path planning. Regarding the reference costs shown in Table 1, the most distinguishable is the required power cost c_1 and since this paper focuses on evaluation of the SOM in traversal cost learning and not on path planning, we select c_1 as the traversal cost weight to demonstrate the possible impact of the prediction traversal cost to navigation of the robot. A path planning is considered for a grid-like environment, where the motion cost from moving from the cell ν_1 to the neighboring cell ν_1 is computed as

$$c(\nu_1, \nu_2) = \frac{c_1(\nu_1) + c_1(\nu_2)}{2} \cdot \|(\nu_1, \nu_2)\|\,, \tag{4}$$

where $c_1(\nu_1)$ and $c_1(\nu_2)$ is the predicted (or reference) required power cost c_1 of the grid cells ν_1 and ν_2, respectively, and $\|(\nu_1, \nu_2)\|$ is the distance between the cells considering 8-neighborhood. Having a grid map of the environment with the traversal cost assessment, the optimal path from the initial location to the goal location can be found by any graph search such as A* or Dijkstra's algorithm.

Fig. 3. Testing grind map of the size 380×30 cells with two terrain types that are hard to traverse: the flat ground covered by black fabric and wooden sloped surface (shown in the red); that are accompanied by the wooden blocks and wooden blocks covered by the black fabric (shown in the blue) that are all placed on the flat ground (shown in the white here to highlight hard to traverse areas).

The robot avoids hard to traverse area if the total cost (using (4)) of traversing the more difficult area is higher than the travel cost of avoiding the area. If the hard to traverse area is small, it might be still optimal to traverse it rather than avoid it. Therefore, an artificial scenario with several hard to traverse areas with the dimensions of the 200×20 grid cells are placed in an environment with a flat ground to form a zig-zag pattern, see Fig. 3. For the map shown in Fig. 3, the optimal path from the grid cell $(0, 10)$ to $(379, 15)$ can be found using the particular traversal cost prediction C_{pred}; however, the final cost path C is determined as the cost over the grid map that is assessed using the reference "*ground-truth*" model $\mathcal{M}_{\text{ref}}$. The assessment for the learned models is performed based on shape and appearance features that are randomly selected from the

Table 4. Average path costs found using traversal cost prediction of c_1

Prediction	**Path Cost**			
model	$\overline{C}$	σ_C	$\overline{\Delta}$ [%]	σ_Δ [%]
$\mathcal{M}_{\text{GP}}^{tt}$	4318.1	18.2	1.5	0.4
$\mathcal{M}_{\text{GP}}$	4259.2	5.7	0.2	0.1
$\mathcal{M}_{\text{SOM}_3}^{10\times10}$	4281.8	23.9	0.7	0.6
$\mathcal{M}_{\text{clustering}}$ - classification	4325.2	23.2	1.7	0.5
$\mathcal{M}_{\text{SOM}}^{10\times10}$-classification	4494.7	9.2	5.7	0.2

Δ is the difference of the path cost from the reference path cost.

features of the trails with the corresponding terrain types, and 20 grids with randomly chosen feature descriptors have been created. Thus, the path costs in Table 4 are reported as the average values $\overline{C}$, the standard deviations σ_C, and also as the average percentage difference $\overline{\Delta}$ of the final path cost found using the predicted traversal cost from the cost of the optimal reference path found using the $\mathcal{M}_{\text{ref}}$ traversal cost model with the standard deviation denoted σ_Δ. Selected found path with the corresponding path costs are depicted in Fig. 4.

(a) Optimal path found with the "*ground-truth*" $\mathcal{M}_{\text{ref}}$, $C = 4252.54$

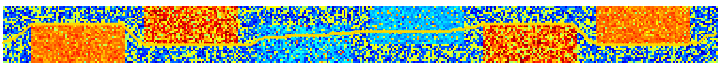

(b) $\mathcal{M}_{\text{GP}}^{tt}$, $C_{pred} = 4415.52$, and $C = 4289.13$

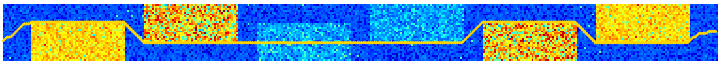

(c) $\mathcal{M}_{\text{GP}}$, $C_{pred} = 4238.54$, and $C = 4252.54$

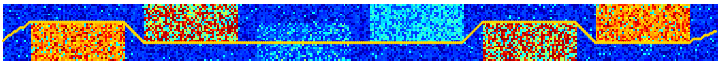

(d) $\mathcal{M}_{\text{SOM}_3}^{10\times10}$, $C_{pred} = 4349.1$, and $C = 4252.54$

Fig. 4. Selected best found optimal paths using different traversal cost model of the cost c_1 (required power) with the predicted cost C_{pred} and the final path cost C computed using the reference traversal costs.

Both $\mathcal{M}_{\text{GP}}$ and SOM-based traversal cost predictions are capable of determining the same solution as the optimal reference path using $\mathcal{M}_{\text{ref}}$ with a lower standard deviation of the GP-based model. The compound $\mathcal{M}_{\text{GP}}^{tt}$ is not able to provide the same solution as the reference model $\mathcal{M}_{\text{ref}}$ in any of the twenty generated grid maps. The maps are randomly created, and also particular features vary in real observations. Therefore, the single reported case does not necessarily mean the compounded model is not a suitable predictor of the traversal costs,

especially when the overall difference of the path cost is about 1.5% of the reference optimal path costs for the model $\mathcal{M}_{\text{ref}}$. Notice, the last two rows in Table 4 is for the predictions using classification based on the identified terrains, which is described in the following section.

4.2 Terrain Types Identification

Unsupervised clustering has been firstly performed for the feature descriptors of the trail $\mathcal{T}_{all}$ to compute the terrain type ratio (3) and study differences between the human labeled terrain types and identified types from the data. Even though the trail is composed of seven terrain types, the smallest cluster separation measure [3] is achieved for six clusters. The corresponding distribution of the labeled terrain types among these clusters is depicted in Table 5.

Table 5. Terrain type ratios of the clustered feature descriptors of $\mathcal{T}_{all}$

Cluster	*flat floor covered by black fabric*	*wooden blocks covered by black fabric*	*wooden blocks*	*wooden blocks covered by artif. turf*	*flat floor*	*wooden sloped surface*	*flat floor covered by artif. turf*
1	1.5	21.5	2.2	0.2	14.0	0.2	0.3
2	0	0	18.7	0	0	1.9	0
3	0	0	0	6.5	0	0	12.2
4	16.4	0	0	0	0	0.2	0.5
5	0	0	0	0	0	3.5	0
6	0	0	0	0	0	0.2	0

The largest cluster includes almost 40% of the features, and the results indicate that *wooden blocks covered by black fabric* might be considered similar to the *flat floor*, which is not expected behavior. The wooden blocks terrain type is identifiable in the second cluster. The third cluster indicates that probably the appearance features are significant for the artificial turf, which is green. The flat floor covered by the black fabric is dominant in the fourth cluster. Finally, two additional clusters cover the wooden sloped surface. The means of the determined clusters can be utilized for the classification with the prediction of the traversal cost determined as the means of the particular cluster traversal cost. However, regarding the results for such $\mathcal{M}_{\text{clustering}}$ in Table 4, the terrain distinguishability is lower than for the traversal cost regression.

The terrain type ratios of clustered learned prototypes from the 10×10 large SOM are depicted in Table 6 and corresponding U-matrix is visualized in Fig. 5. In this case, the smallest separation measure is for eight clusters, and we can read from the results that black fabric is dominant for the first cluster while the artificial turf is dominant for the second cluster. The wooden blocks might be considered similar to the wooden sloped surface. Similarly to Table 5, the wooden sloped surface can be found in several clusters.

Having clustered SOM prototypes, individual costs per each cluster can be computed as the average cost value among the cluster, that can be then utilized

Table 6. Terrain type ratios of the clustered prototypes of the learned $\mathcal{M}_{\text{SOM}}^{10\times10}$

Cluster	*flat floor covered by black fabric*	*wooden blocks covered by black fabric*	*wooden blocks*	*wooden blocks covered by artif. turf*	*flat floor*	*wooden sloped surface*	*flat floor covered by artif. turf*
1	17	15	2	0	6	0	2
2	0	0	0	6	0	0	12
3	0	0	13	0	0	5	0
4	0	0	0	3	0	0	6
5	0	0	0	0	0	6	0
6	0	0	0	2	0	1	0
7	0	0	0	0	0	2	0
8	0	0	0	0	0	2	0

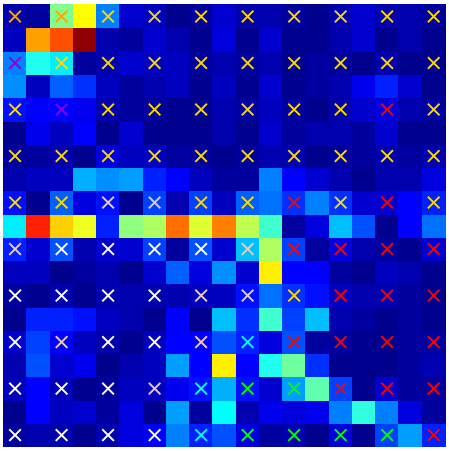

Fig. 5. Visualization of the clustered learned SOM on top of the U-matrix. The individual clusters are shown as small color crosses at the centers of cells corresponding to the prototypes of the SOM lattice.

for traversal cost assessment based on classification of the feature descriptor $\boldsymbol{d}_{sa}$ according to the closest prototype of the learned SOM. Regarding the overview of the path cost in Table 4, such a traversal cost prediction is noticeably worse than the SOM-based regression. However, terrain type identification can be suitable in the scenario where the "*ground-truth*" reference traversal costs are not available because of missing explicit terrain type labels.

4.3 Discussion

The reported results support the feasibility of using SOM for unsupervised learning of the traversal cost model and even relatively small lattice with the size

10×10 provides competitive results to significantly more demanding GP. Moreover, SOM also provides a straightforward prediction of multi-dimensional cost indicators. Although only a relatively simple evaluation of the traversal cost prediction in path planning has been performed, the results support sufficient distinguishability of the hard to traverse areas that can be achieved even for predictors with relatively low correctness ratios. It is especially important in the cases where the reference traversal costs are not explicitly available, e.g., because of a priory unknown environments in robotic exploration missions [12]. SOM-based unsupervised learning can be considered as a suitable technique for traversal cost learning, and we further plan to consider on-line variants of SOM such as [14] to follow the motivational deployments with incremental learning.

Moreover, based on the reported results, we can observe that the robot can perceive the terrain differently than the natural labels derived from the particular terrains the robot traversed. It is also because the proprioceptive sensing can be similar for two terrains that can appear differently, e.g., like wooden blocks and a wooden sloped surface which are different mainly in shape features but look similar in ab channels of the Lab color space. Hence, we can speculate that the human labels for the terrain types might be misleading, albeit they seem to be a natural choice, which is used for learning the reference model $\mathcal{M}_{\text{ref}}$ and also the compounded GP-based model $\mathcal{M}^{tt}_{\text{GP}}$. The most important part of the "*ground-truth*" is the fact that in the motivational deployment of the robot in a priory unknown environment, the explicit labels are not available, and the robot has to rely solely on unsupervised learning, where the most important quality measure is a sufficient distinguishability of the hard to traverse areas regarding the particular cost. The presented results indicate that a combination of several traversal costs is probably necessary, as considering a single cost might now provide sufficient distinguishability. The evaluation of the traversal cost predictors in such setups is considered as a subject of our future work.

5 Conclusion

In this paper, we report on unsupervised learning of robot traversal cost predictors. The results support that SOM can provide competitive predictions to the GP-based model, but it is less computationally demanding. Moreover, the unsupervised terrain types identification provides a different view on the natural human labels of the terrains, and it seems to be suitable to focus on how the terrain types are perceived by the robot rather than human labeling, which is particularly important in the deployments without known terrain types. Besides, the results further support that prediction based on the weighted average from the closest prototypes improves the predicted values concerning the reference model. However, there is still an open question of how the predictors for incremental and unsupervised learning should be evaluated because of the stochastic nature of the cost variables and also the exteroceptive features. Therefore, we plan to investigate the alternative feature descriptors and further ways how to create the reference model in addition to improving the predictors.

References

1. Arthur, D., Vassilvitskii, S.: K-means++: The advantages of careful seeding. In: Eighteenth Annual ACM-SIAM Symposium on Discrete Algorithms (SODA). pp. 1027–1035 (2007)
2. Bartoszyk, S., Kasprzak, P., Belter, D.: Terrain-aware motion planning for a walking robot. In: International Workshop on Robot Motion and Control (RoMoCo). pp. 29–34 (2017). doi: 10.1109/RoMoCo.2017.8003889
3. Davies, D.L., Bouldin, D.W.: A Cluster Separation Measure. IEEE Transactions on Pattern Analysis and Machine Intelligence **PAMI-1**(2), 224–227 (Apr 1979). doi: 10.1109/TPAMI.1979.4766909
4. Faigl, J., Prágr, M.: Incremental traversability assessment learning using growing neural gas algorithm. In: Advances in Self-Organizing Maps, Learning Vector Quantization, Clustering and Data Visualization. pp. 166–176 (2020). doi: 10.1007/978-3-030-19642-4_17
5. Faigl, J., Čížek, P.: Adaptive locomotion control of hexapod walking robot for traversing rough terrains with position feedback only. Robotics and Autonomous Systems **116**, 136–147 (2019). doi: 10.1016/j.robot.2019.03.008
6. GPy: A Gaussian process framework in python. `http://github.com/SheffieldML/GPy` (since 2012), cited on 2019-03-28
7. Hartigan, J.A., Wong, M.A.: A k-means clustering algorithm. JSTOR: Applied Statistics **28**(1), 100–108 (1979). doi: 10.2307/2346830
8. Kohonen, T.: Self-organizing maps. Springer, 3rd edn. (2001)
9. Kragh, M., Jørgensen, R.N., Pedersen, H.: Object detection and terrain classification in agricultural fields using 3d lidar data. In: Int. Conf. Computer Vision Systems (ICVS). vol. 9163, pp. 188–197 (2015). doi: 10.1007/978-3-319-20904-3_18
10. Prágr, M., Čížek, P., Faigl, J.: Cost of transport estimation for legged robot based on terrain features inference from aerial scan. In: IEEE/RSJ Int. Conf. Intelligent Robots and Systems (IROS). pp. 1745–1750 (2018). doi: 10.1109/IROS.2018.8593374
11. Prágr, M., Čížek, P., Faigl, J.: Incremental learning of traversability cost for aerial reconnaissance support to ground units. In: Modelling and Simulation for Autonomous Systems (MESAS). pp. 412–421 (2019). doi: 10.1007/978-3-030-14984-0_30
12. Prágr, M., Čížek, P., Faigl, J.: Online incremental learning of the terrain traversal cost in autonomous exploration. In: Robotics: Science and Systems (RSS) (2019). doi: 10.15607/RSS.2019.XV.040
13. Rasmussen, C.E., Williams, C.K.I.: Gaussian Processes for Machine Learning. MIT Press (2006)
14. Rougier, N., Boniface, Y.: Dynamic self-organising map. Neurocomputing **74**(11), 1840–1847 (2011). doi: 10.1016/j.neucom.2010.06.034
15. Ultsch, A., Siemon, H.P.: Kohonen's self organizing feature maps for exploratory data analysis. In: Intl. Neural Network Conference (INNC). pp. 305–308 (1990)
16. Vasudevan, S., Ramos, F., Nettleton, E., Durrant-Whyte, H., Blair, A.: Gaussian Process modeling of large scale terrain. In: IEEE Int. Conf. Robotics and Automation (ICRA). pp. 1047–1053 (2009). doi: 10.1002/rob.20309
17. Vesanto, J., Alhoniemi, E.: Clustering of the self-organizing map. IEEE Transactions on Neural Networks **11**(3), 586–600 (2000). doi: 10.1109/72.846731
18. Čížek, P., Faigl, J.: On localization and mapping with rgb-d sensor and hexapod walking robot in rough terrains. In: IEEE Intl. Conf. Systems, Man, and Cybernetics (SMC). pp. 2273–2278 (2016). doi: 10.1109/SMC.2016.7844577